Resonant-Raman-scattering study on short-period Si/Ge superlattices

R. Schorer and G. Abstreiter
Walter Schottky Institut, Technische Universität München, Am Coulombwall, D-85748 Garching, Germany

H. Kibbel and H. Presting
Daimler-Benz AG, Research Center Ulm, Wilhelm-Runge-Strasse 11, D-89081 Ulm, Germany
(Received 22 August 1994)

Resonant Raman scattering is performed between 1.6 and 3.0 eV on a series of strain-symmetrized $(Si)_n(Ge)_n$ superlattices with $n=4-12$ and a $(Si)_4(Ge)_{12}$ superlattice pseudomorphic to the Ge substrate. The dependence of the resonance energies and the degree of localization of states on single-layer thickness and strain are investigated. The results are compared with band-structure calculations and electroreflectance results on similar samples. We observe strong transitions confined within the Ge layers below 2.5 eV and transitions that are attributed to the intermixed interface regions, since they appear independently of layer thickness for all phonon modes around 2.6 eV. The shift of the dominant Ge-like transitions with layer thickness is much weaker than calculated for the localized E_0 superlattice transitions. These resonance maxima cannot be explained by bulk Ge-like E_1 transitions, since their energy is below E_1 of strained bulk Ge. Folded acoustic modes show a pronounced upward shift of the energy of the resonance maximum with increasing mode index. Forbidden confined LO_m modes with even index m were observed under resonance conditions in nonpolar superlattices.

I. INTRODUCTION

The main interest on the electronic band structure of Si/Ge superlattices (SL's) has been focused on the fundamental band gap which is crucial for optoelectronic applications and can be studied by luminescence or absorption experiments. Although there are numerous theoretical investigations on higher electronic transitions, systematic experimental studies in this field are rather rare. Such experiments were mainly performed by modulation spectroscopy, namely, by photoreflectance,[1] electroreflectance,[2–5] and piezoreflectance.[6] These techniques are simple and sensitive and allow an accurate determination of the energies of optical transitions, but they often require a special sample design with respect to doping and layer thicknesses. Extrinsic effects like Franz-Keldysh or interference oscillations may strongly contribute to spectra, which created some controversaries about the interpretation of experimental results.[6] The dielectric function of Si/Ge SL's was determined by means of ellipsometry for energies above 2 eV.[7]

Modulation spectroscopy and ellipsometry do not distinguish between localized and extended states. The main feature of resonant Raman scattering (RRS) on SL's is that due to phonon-confinement effects information on the degree of the spatial localization of electronic states can be obtained. Therefore RRS is an interesting complementary technique to modulation spectroscopy, although the determination of transition energies is less accurate. The phonons in Si/Ge SL's can be localized either in the Si or Ge layers (optical modes) or extended through the whole structure (acoustic modes). Maxima of the Raman cross section of each mode are expected, whenever the energy of the incident or scattered light coincides with transitions between electronic states which are modulated by the particular phonon mode. Thus confined Ge-like (Si-like) modes should not couple to electronic states localized within the Si (Ge) layers.

Although various RRS studies have been performed on III/V-based SL's, only little data exist for Si/Ge SL's.[8,9] In Ref. 9 SL's grown pseudomorphically to Ge substrate were investigated. The Si layer thickness was limited to 4 ML's. Results are in reasonable agreement with photoreflectance measurements on the same samples. Cerdeira *et al.*[8] performed RRS on SL's on relaxed alloy buffers. Both works show clear evidence of a localization of electronic states in the Ge layers. Since only a very small number of samples was investigated, a systematic study of the dependence of RRS features on structural sample parameters like strain and single-layer thickness was still lacking. In this paper we will present RRS results of a series o strain-symmetrized Si_nGe_n SL's with $n=4-12$ where only the SL period $2n$ was varied. For comparison a $(Si)_4(Ge)_{12}$ SL pseudomorphic to Ge substrate and a fully relaxed $(Si)_3(Ge)_7$ were investigated as well. Results are compared with electronic band-structure calculations.

II. EXPERIMENTAL DETAILS

$(Si)_n(Ge)_n$ SL's with $n=4$, 5, 6, 8, and 12 were grown by molecular-beam epitaxy on a partially relaxed 20-nm $Si_{0.25}Ge_{0.75}$ alloy buffer layer on a (001)-Si substrate. The flux rates were ≈ 0.3 Å/sec. The strain-symmetrizing sample design prevents relaxation even for large SL thickness which were between 200 and 500 nm in our case. Part of the samples was characterized by x-ray diffraction. Good interface quality was achieved by low growth temperatures of ≈ 310 °C and by the use of the Sb surfactant technique.[10] As a consequence of the latter,

the samples are n doped. A fully relaxed $(Si)_3(Ge)_7$ SL with a thickness of 1 μm was grown on top of a thin Ge buffer on a (001)-Si substrate. A thin 34-nm $(Si)_4(Ge)_{12}$ SL was grown pseudomorphic to Ge substrate.

The RRS measurements were performed in conventional backscattering from the growth surface, where sample heating was avoided by the use of a cylindrical lens for focusing the light. All measurements were performed at room temperature or at ≈ 80 K in a liquid-nitrogen cold-finger cryostat. For excitation various lines of an Ar^+, Kr^+, and a dye laser with Styril8, DCM, Rhodamine 6G, and Rhodamine 110 dyes were used. The signal was dispersed by a triple grating spectrometer (1800 lines/mm) with a focal length of 0.5 m used in the subtractive mode. The spectral resolution was between 2 and 4 cm^{-1}. The signal was detected with a cooled charge-coupled device camera. For each wavelength a reference signal was recorded from a bulk Si sample having the same orientation, which was mounted beneath the SL samples. With this technique, the Raman efficiency of the SL is given by[11]

$$S_{SL}=S_{Si}\frac{S^*_{SL}}{S^*_{Si}}\frac{1}{1-e^{-2\cdot\alpha_{SL}\cdot d_{SL}}}\frac{\alpha_{Si}n^2_{Si}}{\alpha_{SL}n^2_{SL}}\left[\frac{1-R_{Si}}{1-R_{SL}}\right]^2. \quad (1)$$

S^*_{SL} and S^*_{Si} are the intensities of the Si and SL signal measured in the RRS experiment, S_{Si} is the known Raman efficiency of Si,[12] α_{Si}, n_{Si}, and R_{Si} are the absorption, refractive index, and reflectivity which were taken from Ref. 13. d_{SL} denotes the SL total thickness. R_{SL} was directly measured for each SL sample, since pronounced interference oscillations are present for all samples below ≈ 2.4 eV. n_{SL} was estimated by $(n_{Si}+n_{Ge})/2$. α_{SL} was estimated by the intensity ratio between the Si reference signal and the signal S^*_{sub} from the Si substrate of the SL's which is observable below ≈ 2.4 eV:

$$\alpha_{SL}=\frac{1}{2d_{SL}}\left\{\ln\left[\frac{S^*_{Si}(1-R_{SL})^2}{S^*_{Sub}(1-R_{Si})^2}\right]-2\alpha_{Buf}d_{Buf}\right\}, \quad (2)$$

where d_{Buf} is the alloy buffer-layer thickness. The absorption α_{Buf} of the buffer layer was taken from Ref. 13. At 3 eV, $\alpha_{SL}=\alpha_{Ge}$ was assumed for all samples.[8] In the energy region where no Si substrate signal could be detected (≈ 2.4–3 eV), the absorption was interpolated. Although the determination of the absorption with this technique is not very accurate, the peak positions in the Raman resonance curves are only weakly affected by this uncertainty. The labeling of the axes z [001] (growth axis), x [100], y [010], and x' [1$\bar{1}$0] refers to the conventional cubic unit cell of the bulk materials.

III. EFFECTS OF LAYER THICKNESS

Figure 1 shows Raman spectra of the $(Si)_n(Ge)_n$ SL's and the corresponding alloy, measured at 2.54 eV in $z(x',x')\bar{z}$ polarization. Both longitudinal-optical (LO) and -acoustic modes are Raman active. For the $(Si)_4(Ge)_4$ SL and for the alloy at 520 cm^{-1} a LO Si signal from the substrate is observed. For $n>4$ around 500 cm^{-1} confined LO_1 and LO_3 Si-like modes appear which are

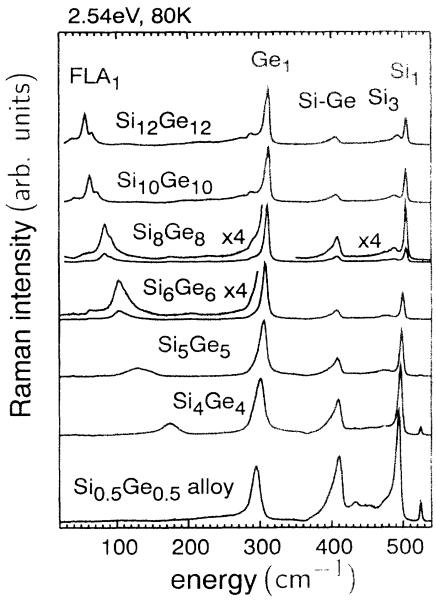

FIG. 1. Raman spectra of various strain-symmetrized $(Si)_n(Ge)_n$ SL's and a $Si_{0.5}Ge_{0.5}$ alloy, recorded 2.54 eV at 80 K in $z(x',x')\bar{z}$ polarization. Intensities are normalized to the Ge_1 mode intensity.

discussed in detail elsewhere.[14] The LO_1 Ge-like mode is present at 300 cm^{-1}. The confinement effect on the optical modes is responsible for its downward shift in energy with decreasing single-layer thickness. The intensity ratio between Si- and Ge-like modes depends pronouncedly on the SL period length. Around 400 cm^{-1} a mechanical LO interface mode appears due to interface intermixing which is discussed in Ref. 15. Signals due to folded acoustic modes, especially the doublet split first-folded longitudinal-acoustic (FLA_1) mode, are detected below 250 cm^{-1}. Below FLA_1 a weak signal is observed for the SL samples, which is ascribed to the forbidden FTA_1 mode.[16]

In Fig. 2 the Raman efficiencies for phonon modes of the $(Si)_8(Ge)_8$ SL as obtained from Eq. (1) are displayed from 1.6 to 3.0 eV at room temperature. At about 2.2 eV a pronounced resonance enhancement of the Ge_1 mode is observed. The resonance maximum is close to the energy of the E_1 transition in bulk Ge. Since the Si_1 mode has the same symmetry as Ge_1, but does not participate in this resonance, the electronic states responsible for the resonance enhancement at 2.2 eV have to be completely localized in the Ge layers. The Raman efficiency for the Si_3 mode, however, shows a clear shoulder near the Ge_1 resonance maximum. This behavior can be explained by the fact that the Si_3 mode, in contrast to the Si_1 mode, penetrates into the intermixed interface layers, as was shown by calculations of the local density of states.[15] Thus a weak coupling of the Si_3 mode to electronic states in the Ge layers is enabled. In the same way the interface mode which is localized in the alloyed interface layers couples to electronic states in the Ge layers, which results in a resonance enhancement at about 2.2 eV. The reso-

nance behavior of the FLA_1 mode is very similar to the Ge_1 mode, since acoustic modes can propagate throughout Si and Ge layers. For all modes a second, weaker resonance enhancement around 2.7 eV is observed. Hence the electronic states related to this resonance are either delocalized or localized at the interface region in which all modes have at least a small amplitude.

Figure 3 shows Raman efficiencies of the Ge_1, Si_1, and FLA_1 mode and the interface more for all $(Si)_n(Ge)_n$ SL's and the alloy obtained in $z(x',x')\bar{z}$ polarization. The most pronounced feature for the Ge_1 mode is a structure evolving from the weak resonance enhancement at about 2.3 eV observed for the alloy phonons, which may be attributed to E_0 transitions. The intensity is drastically increasing and the resonance maximum is slightly shifting downwards in energy with increasing SL period length. For $n=12$ this structure is approaching the energy of the E_1 transition of bulk Ge. A second, weaker structure in the Raman efficiency appears around 2.4 eV for the SL's which has a maximum strength for $n=6$. A third peak around 2.7 eV is present for all samples with similar strength and position. It is attributed to alloylike E_1 transitions in the intermixed interface region. Interface roughness for our samples can be modeled by 2–3 alloy ML's at each interface.[14,15]

From the Raman efficiency of the Si_1 mode it is evident that the resonance enhancement of the Ge_1 mode below 2.5 eV is related to electronic states strictly localized in the Ge layers, since no resonance enhancement is observed for the Si_1 mode in this energy region. A pronounced maximum around 2.7 eV is found both for the alloy and the SL samples. Hence this structure is also related to alloylike transitions at the interfaces. Consequently, the resonance around 2.7 eV is also observed for the Si-Ge interface mode. In contrast to the Si_1 mode, the Si-Ge mode can couple to localized electronic states in the Ge layers due to its localization at the interfaces, giving additional rise to the peak near 2.2 eV. Note that already for the $(Si)_4(Ge)_4$ SL the localization of electronic states in the Ge layers is evident from comparing Ge_1 and

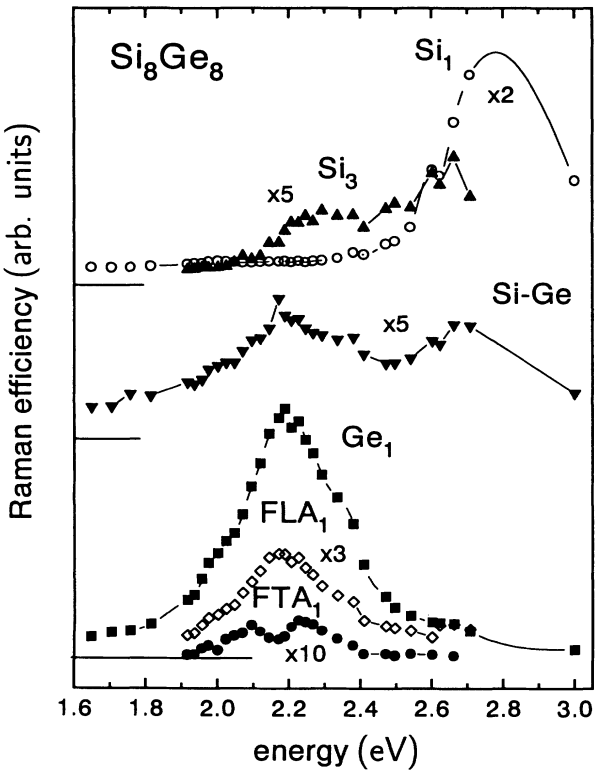

FIG. 2. Raman resonance curves at 300 K for various phonon modes of a strain-symmetrized $(Si)_8(Ge)_8$ SL.

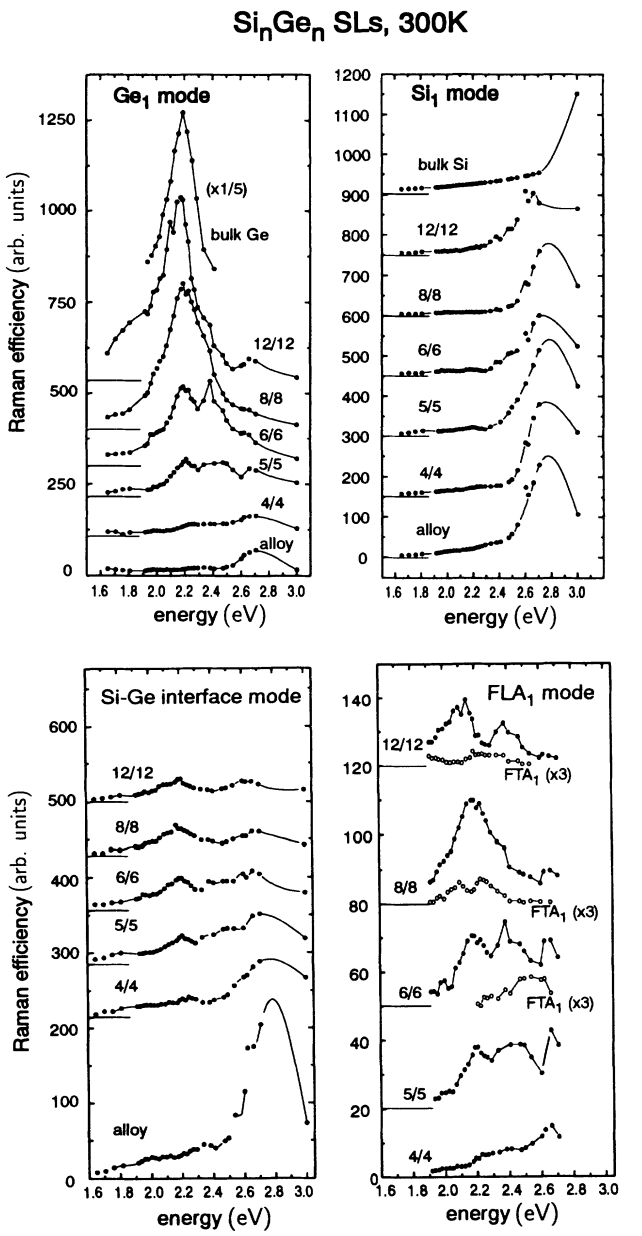

FIG. 3. Room-temperature Raman efficiency of the Ge_1, Si_1, Si-Ge interface, FLA_1, and FTA_1 modes of various strain-symmetrized $(Si)_n(Ge)_n$ SL's, a $Si_{0.5}Ge_{0.5}$ alloy, and a bulk Ge reference. The Raman efficiencies are in arbitrary units, but can be compared with each other for each mode.

Si_1 Raman efficiencies around 2.4 eV. This is consistent with theoretical results for ideal Si/Ge SL's, where for $n > 4$ a formation of bulklike electronic states is expected.[17]

Since the FLA_1 mode propagates through Si and Ge layers, a resonance enhancement is observed both at 2.2 and 2.7 eV. In Fig. 3 also the resonance curves of the FTA_1 mode are depicted. The measured Raman efficiencies are qualitatively similar to that observed for the FLA_1 mode. If the appearance of the forbidden FTA_1 mode is due to forward scattering of light reflected at the interfaces, as suggested in Ref. 16, the intensity should increase with decreasing absorption, i.e., decreasing energy. Since this general energy dependence is expected to be superimposed by resonances, the RRS results are not in contradiction to the suggested scattering mechanism for the FTA_1 mode.

In Fig. 4 the energy positions of the dominant structures in the Raman efficiencies of the Ge_1 mode from Fig. 3 are plotted versus period length. The following main features of Si/Ge SL's interband transitions are expected. Theoretical work showed that SL interband transitions can be discussed to certain extent in terms of E_0 and E_1-like transitions derived from the bulk materials.[17–20] For Si/Ge SL's at the Γ point only transitions between the three topmost valence-band states and a single conduction-band state which consists of bulk Ge Γ states are strong. For increasing SL period these states become completely localized in the Ge layers. Consequently, the E_0 transition energy is continuously lowered from 2.3 eV for a $Si_{0.5}Ge_{0.5}$ alloy to 0.9 eV (bulk Ge) for SL's with very thick Ge layers. The hollow triangles in Fig. 4 denote strong E_0 transitions as obtained from tight-binding calculations.[21] The E_1 transitions of the bulk materials turn into a multiplet structure for the SL's due to the reduced crystal symmetry, giving rise to various peaks in ellipsometry and electroreflectance (ER) spectra of SL's.[5,19] The calculated dominant E_1 transition is denoted by asterisks.[7] In contrast to the E_0 states, the E_1-like states are expected to be delocalized for short periods.[18] For long periods, however, the states become localized in Si and Ge layers. Starting from an energy of 2.7 eV for the alloy, the E_1 transitions thus split into Si- and Ge-like transitions which approach the bulk values for very large period lengths. The energy dependence on the SL period is expected to be weaker than for E_0 due to weaker localization of the corresponding states.

From Fig. 4 the assignment of the peaks seems clear only for $n \leq 6$. The maxima in the Raman efficiencies of the alloy phonons correspond to E_0 and E_1 transitions.[8] For the SL's with $n \leq 6$ the resonance peak with the lowest energy falls in the energy range of the calculated E_0 transitions, whereas the peaks 0.3 eV above are close to the calculated dominant E_1 transitions. The resonance maximum observed for all samples at about 2.7 eV is attributed to an alloylike E_1 transition at the intermixed interfaces. The latter assignment remains valid also for larger periods, whereas the energy shift of the dominant resonance maximum for the Ge_1 mode at about 2.2 eV with period length is much weaker than the energy shift

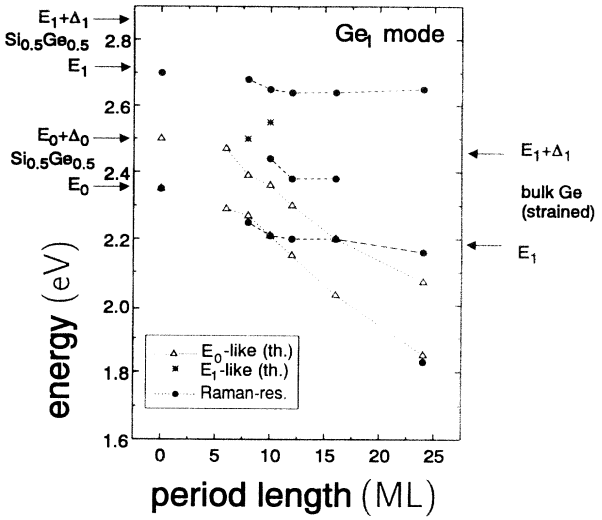

FIG. 4. Measured energies of Raman resonance peaks of the Ge_1 mode of $(Si)_n(Ge)_n$ SL's vs period length $2n$ (full symbols), together with calculated E_0 (triangles) (Ref. 21) and E_1-like transition energies (asterisks) (Ref. 7). The $Si_{0.5}Ge_{0.5}$ alloy is plotted at "0."

of the E_0 transitions predicted by theory. On the other hand, there are arguments against an assignment of this dominant structure to E_1-like transitions.

(1) The observed resonance is completely localized in the Ge layers, whereas states involved in E_1-transitions should be rather delocalized for short period SL's.

(2) The energy of the maximum is *below* the calculated E_1 and $E_1+\Delta_1$ transitions for bulk Ge strained biaxially by 2%.[20] In any case the SL E_1 transitions should be *above* the E_1 energy of bulk Ge. In case of localization the energy of the states is increased by confinement; in case of delocalization the energy is increased by an admixture of Si-like wave-function components, since the E_1 transition of bulk Si is at 3.4 eV.

This is confirmed by ellipsometry measurements on similar short-period $(Si)_n(Ge)_n$ SL's where a maximum shift of the dominant E_1 transition of only 0.2 eV compared to the corresponding $Si_{0.5}Ge_{0.5}$ alloy was found.[19]

Further evidence for the assumption that the RRS maxima around 2.2 eV are not related to E_1 transitions is given in Fig. 5 where the Raman efficiencies of a fully relaxed $(Si)_3(Ge)_7$ SL are compared with the energies of the E_1 transitions of this sample determined by ellipsometry.[7] The resonance enhancement of the Ge_1 mode at 2.2 eV is more than 0.3 eV below the E_1 transition at 2.49 eV. Only the maximum of the Si mode efficiency and a weak shoulder of the Ge_1 mode efficiency seem to be related to the E_1 transition.

The weak shoulder in the Raman efficiency of the Ge_1 mode observed at 1.8 eV for the $(Si)_{12}(Ge)_{12}$ SL falls exactly within the expected energy range of the E_0 transitions. However, a corresponding structure for the $(Si)_8(Ge)_8$ SL could not be found.

RRS on SL's pseudomorphic to Ge substrate with very

thin Si layers (≤ 4 ML) was performed by Menczigar, Eberl, and Abstreiter.[9] A resonance enhancement observed below 2.2 eV for the Ge-like modes could be attributed to E_0-like transitions between electronic states localized in the Ge layers. The Raman efficiencies measured in the energy range of the E_0 transitions were weaker than in the energy range of E_1 alloylike transitions around 2.5 eV. Only for a partially relaxed $(Si)_3(Ge)_9$ SL a dominant E_0 SL transition was found. A RRS study on $Si/Si_{1-x}Ge_x$ SL's showed resonances localized in the alloy layers with energies between E_0 and E_1 of the *bulk* alloys.[22] Consequently these resonances were attributed to E_0-like transitions with an energy increased by confinement in the alloy layers.

An ER study on similar SL samples as investigated in the present work revealed E_0 transitions with an energy continuously shifted from 2.3 eV for $n=4$ to 1.5 eV for $n=16$, which is in good agreement with theory.[5] Between 2.3 and 3.3 eV four transitions with an energy only weakly dependent on period length were resolved, which were attributed to split Si- and Ge-like E_1 SL transitions. For $n \geq 8$, however, an additional weak peak with a constant energy slightly below E_1 of 2% strained bulk Ge was detected, which was also attributed to split E_1-like transition. A satellite peak below the expected E_1 transitions was also observed in GaAs/AlAs and $InSb/In_{1-x}Al_xSb$ SL's.[23,24] The energy of the satellite peak measured with ER (Ref. 5) is close to the energy of the dominant RRS maxima of the Ge_1 mode for $n=8$ and 12, if the shift due to different temperatures (80 and 300 K) is considered. The oscillator strength of this transition as derived from the ER spectra, however, is rather small compared to the measured dominant E_1 transitions.

IV. STRAIN EFFECTS

For investigating strain effects on RRS in Fig. 6 Raman efficiencies of the Si_1 and Ge_1 mode are compared for the strain-symmetrized $(Si)_{12}(Ge)_{12}$ SL ($\varepsilon_{Si}=2\%$) and a $(Si)_4(Ge)_{12}$ SL which was grown pseudomorphically to a Ge substrate ($\varepsilon_{Si}=4.1\%$). The Raman efficiency for the $(Si)_4(Ge)_{12}$ SL is enhanced compared with the $(Si)_{12}(Ge)_{12}$ SL, which is partially due to the larger relative Ge volume. The dominant resonance peak is shifted by ≈ 0.2 eV to lower energy for the pseudomorphic SL. As for the $(Si)_{12}(Ge)_{12}$ SL it is evident from the Raman efficiencies of the Si_1 mode that the electronic states connected with the dominant maximum are located in the Ge layers. The weaker resonance maximum around 2.4 eV also appears for the Si_1 mode, which is evidence that the resonance enhancement can be ascribed to E_1-like transitions in the interface regions or in the thin Si layers. The pronounced shift of both resonance maxima to lower energy compared to the corresponding features for the $(Si)_{12}(Ge)_{12}$ is most likely due to the 2% larger in-plane lattice constant of the $(Si)_4(Ge)_{12}$ SL, since the Ge layer thickness is equal in both cases. The E_0 and $E_1+\Delta_1$ transitions of bulk Ge are expected to increase by 160 and 110 meV for 2% biaxial compression, respectively.[20]

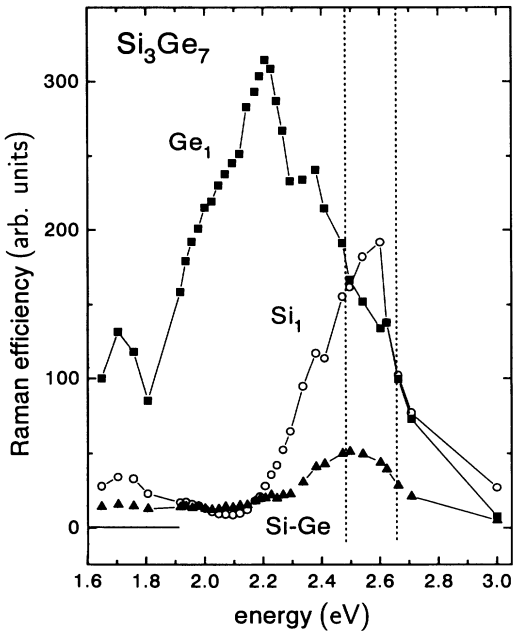

FIG. 5. Raman resonance curves at 300 K for various phonon modes of a fully relaxed $(Si)_3(Ge)_7$ SL. The dashed lines indicate the dominant E_1 transitions of this sample as determined by ellipsometry (Ref. 7).

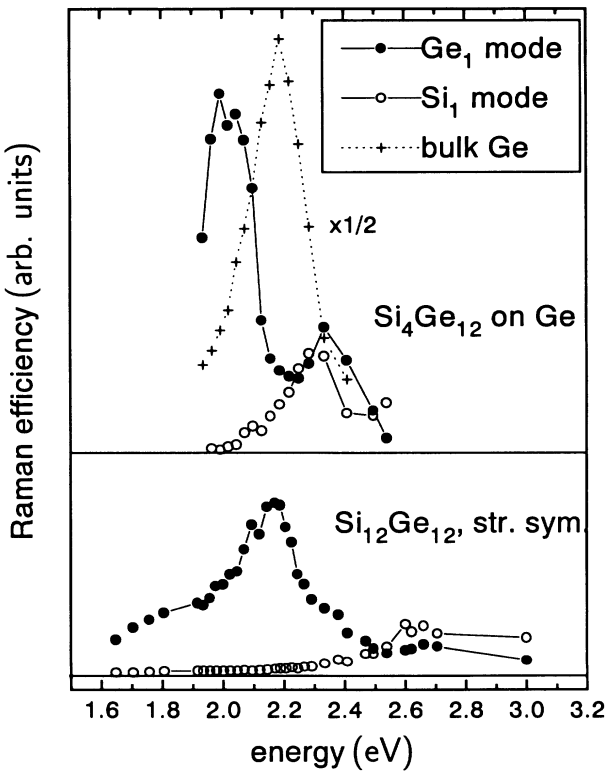

FIG. 6. Raman resonance curves at 300 K for Si_1 and Ge_1 mode of a strain-symmetrized $(Si)_{12}(Ge)_{12}$ SL and a $(Si)_4(Ge)_{12}$ SL pseudomorphic to Ge substrate.

V. ACOUSTIC MODES

Features of RRS of folded acoustic modes will be discussed on the basis of Fig. 7 which shows Raman efficiencies for the FLA modes of the $(Si)_{12}(Ge)_{12}$ SL. As acoustic modes are propagating through the SL structure, a similar resonance enhancement is expected as for the confined optical modes. For the FLA_1 mode a strong resonance enhancement around 2.1 eV is observed close to the dominant resonance maximum of the Ge_1 mode (see Fig. 4). Also the alloylike resonance peak of the Ge_1 mode at 2.6 eV is observed for the FLA_1 mode. Additionally a strong resonance around 2.4 eV is present for the FLA_1 mode, whereas no such structure is found for the Ge_1 mode, see Fig. 4. A possible reason for the appearance of additional features in the Raman efficiencies of acoustic modes is their different symmetry compared with optical modes. Acoustic modes ideally have Γ_1 symmetry. Excitations with Γ_1 symmetry cannot mix different electronic bands which results in a two-band Raman resonance behavior. This symmetry effect leads to a splitting of the single resonance peak in bulk Ge which is observed for 1 LO scattering into two separate E_1 and $E_1+\Delta_1$ peaks for 2TO overtone scattering (overtone scattering also has Γ_1 symmetry).[25] For the confined optical SL phonon modes three-band scattering seems to be dominant, since in Fig. 4 no significant reduction of the full width at half maximum (FWHM) of the resonances compared to the 230 meV width of the bulk Ge E_1 Raman resonance is observed. The dominant FLA_1 resonance is of similar width. The resonance enhancement of the FLA_2, FLA_3, and FLA_4 mode, however, is completely different. An increasing shift of the resonance maximum to higher energy with increasing mode index m is observed. On the other hand, the FWHM of the Raman resonance for the FLA_2 mode is significantly reduced to 130 meV. This might be evidence for a two-band resonance behavior of higher index folded acoustic modes.

The observed energy shift of the resonance maximum might be explained by a simple qualitative argument. The number of nodes of the displacement amplitude of folded acoustic modes is roughly proportional to the mode index m. A strong coupling between phonons and electronic states is likely if the envelopes of the phonon displacement and the electronic wave functions are very similar. An increasing number of nodes for an electronic wave function results in an increasing energy of the corresponding electronic states. Therefore phonon modes with a high index m should couple more strongly to states with higher energy and hence show a resonance maximum at higher energy. In Fig. 7 the energy of the resonance maximum of the folded acoustic modes is continuously increased from FLA_1 to FLA_4 by ≈ 300 meV.

VI. RESONANCE EFFECTS FOR Ge-LIKE MODES

A very interesting effect concerning the selection rules for the Ge-like confined optical modes is observed under resonance conditions. Figure 8 shows Raman spectra of the Ge-like modes of the $(Si)_{12}(Ge)_{12}$ SL recorded in $z(x,x)\bar{z}$ and $z(y,x)\bar{z}$ polarization with different excitation energies at 77 K. For 2.18-eV excitation a significant signal is observed only for depolarized scattering, whereas for excitation at 2.54 and 2.60 eV also for polarized scattering a pronounced signal appears with a maximum which is shifted downwards by about 4 cm^{-1}. Hence for

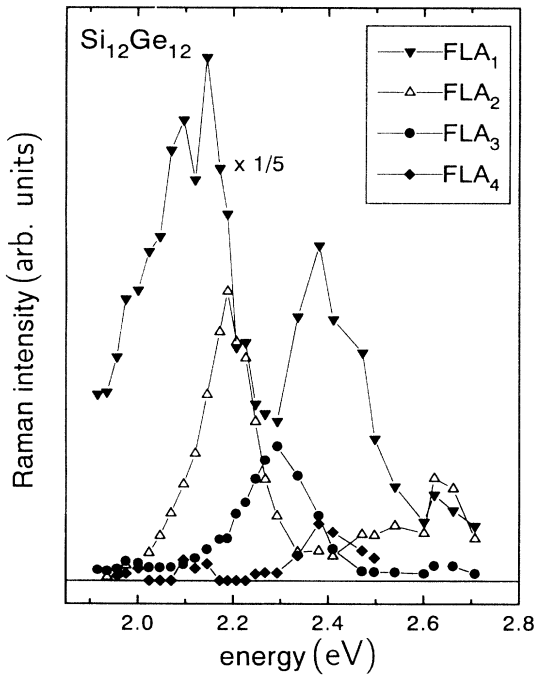

FIG. 7. Raman resonance curves at 300 K for various FLA_m modes of a strain-symmetrized $(Si)_{12}(Ge)_{12}$ SL.

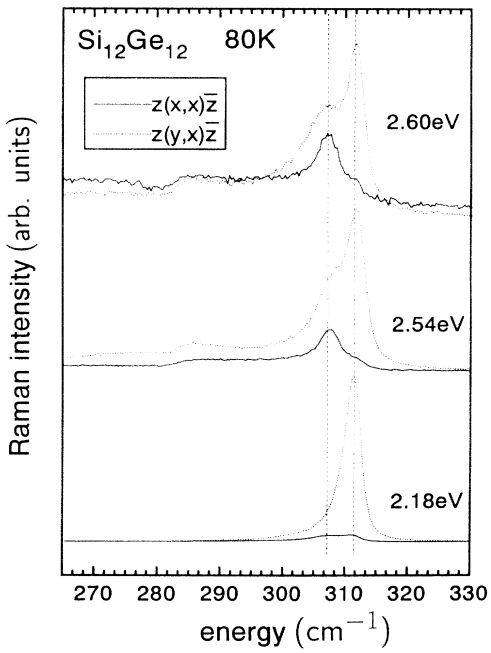

FIG. 8. Raman spectra of the Ge-like confined LO modes of the $(Si)_{12}(Ge)_{12}$ SL recorded with different excitation energies at 80 K in $z(x,x)\bar{z}$ and $z(y,x)\bar{z}$ configuration.

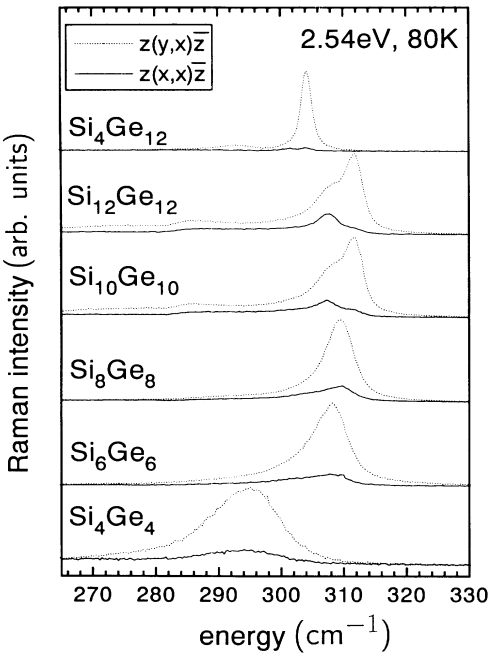

FIG. 9. Raman spectra of the Ge-like confined LO modes of various $(Si)_n(Ge)_k$ SL's recorded at 2.54 eV at 80 K in $z(x,x)\bar{z}$ and $z(y,x)\bar{z}$ configuration. The $(Si)_n(Ge)_n$ SL's are strain symmetrized ($\varepsilon_{Si}=2\%$), whereas the $(Si)_4(Ge)_{12}$ SL is pseudomorphic to Ge substrate ($\varepsilon_{Si}=4.1\%$).

these excitation energies the peak at 308 cm^{-1} is present in both polarizations with comparable strength.

According to the selection rules for deformation potential scattering in $z(y,x)\bar{z}$ LO_m modes with odd index m are allowed, whereas in $z(x,x)\bar{z}$ only Brillouin and folded acoustic modes should be Raman active. LO_m modes with even index m are inactive due to their vanishing overall dipole moment.[26] The dominant signal in $z(y,x)\bar{z}$ at 312 cm^{-1} is attributed to the LO_1 mode. From the selection rules and in analogy to result of the Si-like modes, the shoulder at 308 cm^{-1} should be due to LO_3, since the intensity of confined optical modes is expected to be proportional to $1/m^2$. From the bulk dispersion and from microscopic calculations the LO_3 frequency is expected around 300 cm^{-1} for this sample. This large discrepancy cannot be explained by interface roughness, if the 2-ML intermixing for this sample series derived from the features of the Si-like and Si-Ge modes is modeled in the calculation. From theory frequencies around 308 cm^{-1} are found for LO_2 and TO_1 modes.[27] The 308-cm^{-1} peak cannot be due to disorder-induced non-k-conserving scattering (e.g., density of states contributions), since its line shape is not significantly broadened compared to the allowed LO_1 peak. The appearance of a strong TO_1 mode in backscattering from a (001) surface would require a huge in-plane wave-vector component. No convincing scattering mechanism for this could be identified yet.

For a further discussion in Fig. 9 Raman spectra of $(Si)_n(Ge)_n$ SL's and a $(Si)_4(Ge)_{12}$ SL recorded in $z(x,x)\bar{z}$ and $z(y,x)\bar{z}$ for excitation at 2.54 eV are shown. Only for the $n=10$ SL features similar to $n=12$ are observed. For all other samples in $z(x,x)\bar{z}$ only the entire signal is weakened, but no frequency shifts or additional modes appear. Especially interesting is the comparison to the $(Si)_4(Ge)_{12}$ SL which has the same Ge layer thickness, but much thinner Si layers than the $(Si)_{12}(Ge)_{12}$ SL. For the first sample the selection rules are almost perfectly fulfilled. Hence the peak at 292 cm^{-1} is attributed to LO_3. Only a very weak signal in $z(x,x)\bar{z}$ is observed around 302 cm^{-1} which might be interpreted as LO_2. For such weak signals, however, one has always to take also disordered-induced density of states contributions into account.

The effect that under resonance conditions forbidden LO_m modes with even m gain considerably in intensity is well known for GaAs/AlAs SL's for which these modes even can dominate the odd-numbered allowed modes.[28] In SL's of polar materials this behavior is well understood in terms of scattering via Fröhlich interaction for which even-numbered LO_m modes are Raman active. For unpolar material system like Si/Ge, however, Fröhlich interaction is completely negligible with respect to deformation potential scattering. Consequently, up to now no observation of even-numbered LO_m modes in Si/Ge SL's has been reported.

Obviously the unknown scattering mechanism is *not* symmetry related, since all SL's in Fig. 9 ideally should have orthorhombic symmetry. On the other hand, Fig. 9 gives evidence that the effect is both related to Si *and* Ge layer thicknesses. This is consistent with the observation that the effect is present for excitation energies where the Si_1 mode is resonant (see Fig. 3). This leads to a possible explanation for the appearance of confined Ge-like optical modes in $z(x,x)\bar{z}$. From the calculated atomic displacement pattern it is evident that especially Ge-like LO modes with high index m can have a pronounced acousticlike displacement in the Si layers due to their coupling to the LA bulk Si phonon branch. These acoustic contributions are Raman allowed in $z(x,x)\bar{z}$ and might be rather intense for resonances in the Si layers. This mechanism, however, cannot explain a Raman signal of LO_m modes with even m in $z(y,x)\bar{z}$.

The structure below 290 cm^{-1} for the $n=12$ and $n=10$ SL shows a polarization dependence similar to the 308-cm^{-1} peak and could be attributed to LO_4 according to its frequency. It is to consider, however, that the line shape of this peak is extremely asymmetric. The dip at 280 cm^{-1} is close to the energy where LO and TO Ge bulk dispersion branches cross along [001]. Hence the dip might correspond to a frequency gap in the density of states due to a *anticrossing* of these branches, similar to recent observations of Ruf *et al.*[29] for LA and TA branches in GaAs/AlAs SL's. This *anticrossing*, however, requires in-plane wave-vector component.

VII. CONCLUSION

We have shown that resonant Raman scattering is a sensitive tool for investigating electronic transitions above the fundamental band gap of Si/Ge SL's. Three

resonances are found around 2.2, 2.4, and 2.7 eV. The latter appears for all phonon modes and is attributed to E_1 alloylike transitions in the intermixed interface region. The other resonances are due to states localized in the Ge layers. The layer thickness affects mainly their strength, whereas the dependence of their energetic position is much weaker than expected from theory. Already for a $(Si)_4(Ge)_4$ SL localized states are evident. The dominant resonance at 2.2 eV falls in between the calculated E_0 and E_1 transition energies for $n \geq 8$. This behavior is not understood yet, whereas the observed shift of this resonance with biaxial strain is in agreement with theory. For FLA_m modes the energy position of the resonance maximum is continuously increasing with the mode index m. Confined optical modes were observed under resonance conditions which could not be attributed to the allowed LO_m modes with odd index m.

ACKNOWLEDGMENTS

The authors would like to thank U. Menczigar, G. Theodorou, E. Molinari, T. Ruf, and M. Cardona for many interesting and helpful discussions. The work was financially supported by the EU via ESPRIT Basic Research Project No. P7128.

[1]P. A. Dafesh, V. Arbet-Engels, and K. L. Wang, Appl. Phys. Lett. **56**, 1498 (1990).
[2]T. P. Pearsall, J. Bevk, L. C. Feldman, J. M. Bonar, and J. P. Mannaerts, Phys. Rev. Lett. **58**, 729 (1987).
[3]T. P. Pearsall, J. M. Vandenberg, R. Hull, and J. M. Bonar, Phys. Rev. Lett. **63**, 2014 (1989).
[4]T. P. Pearsall, J. Bevk, J. C. Bean, J. Bonar, J. P. Mannaerts, and A. Ourmazd, Phys. Rev. B **39**, 3741 (1989).
[5]P. A. M. Rodrigues, F. Cerdeira, and M. Cardona, Solid State Commun. **86**, 637 (1993).
[6]Y. Yin, D. Yan, F. H. Pollak, M. S. Hybertsen, J. M. Vandenberg, and J. C. Bean, Phys. Rev. B **44**, 5955 (1991).
[7]U. Schmid, J. Humlícek, F. Lukes, M. Cardona, H. Presting, H. Kibbel, E. Kasper, K. Eberl, W. Wegscheider, and G. Abstreiter, Phys. Rev. B **45**, 6793 (1992).
[8]F. Cerdeira, M. I. Alonso, D. Niles, M. Garriga, M. Cardona, E. Kasper, and H. Kibbel, Phys. Rev. B **40**, 1361 (1989).
[9]U. Menczigar, K. Eberl, and G. Abstreiter, in *Silicon Molecular Beam Epitaxy,* edited by J. C. Bean, E. H. C. Parker, S. S. Iyer, Y. Shiraki, E. Kasper, and K. L. Wang, MRS Symposia Proceedings No. 220 (Materials Research Society, Pittsburgh, 1991), p. 361.
[10]K. Fujita, S. Fukatsu, H. Yaguchi, T. Igarashi, Y. Shiraki, and R. Ito, in *Silicon Molecular Beam Epitaxy* (Ref. 9).
[11]M. Cardona, in *Light Scattering in Solids II,* edited by M. Cardona and G. Güntherodt (Springer, Berlin, 1982), p. 19.
[12]J. B. Renucci, R. N. Tyte, and M. Cardona, Phys. Rev. B **11**, 3885 (1975).
[13]J. Humlicek, M. Garriga, M. I. Alonso, and M. Cardona, J. Appl. Phys. **65**, 2827 (1989).
[14]R. Schorer, G. Abstreiter, S. de Gironcoli, E. Molinari, H. Kibbel, and H. Presting, Phys. Rev. B **49**, 5406 (1994).
[15]S. de Gironcoli, E. Molinari, R. Schorer, and G. Abstreiter, Phys. Rev. B **48**, 8959 (1993).
[16]M. I. Alonso, F. Cerdeira, D. Niles, M. Cardona, E. Kasper, and H. Kibbel, J. Appl. Phys. **66**, 5645 (1989).
[17]C. G. van de Walle and R. M. Martin, Phys. Rev. B **34**, 5621 (1986).
[18]S. Froyen, D. M. Wood, and A. Zunger, Phys. Rev. B **37**, 6893 (1988).
[19]U. Schmid, N. E. Christensen, M. Alouani, and M. Cardona, Phys. Rev. B **43**, 14 597 (1991).
[20]C. Tserbak, H. M. Polatoglou, and G. Theodorou, Phys. Rev. B **47**, 7104 (1993).
[21]G. Theodorou, H. M. Polatoglou, and C. Tserbak (unpublished).
[22]F. Cerdeira, A. Pinczuk, and J. C. Bean, Phys. Rev. B **31**, 1202 (1985).
[23]M. Garriga, M. Cardona, N. E. Christensen, P. Lautenschlager, T. Isu, and K. Ploog, Phys. Rev. B **36**, 3254 (1987).
[24]F. Cerdeira, A. Pinczuk, T. H. Chiu, and W. T. Tsang, Phys. Rev. B **32**, 1390 (1985).
[25]M. A. Renucci, J. B. Renucci, R. Zeyher, and M. Cardona, Phys. Rev. B **10**, 4309 (1974).
[26]P. Molinàs i Mata, M. I. Alonso, and M. Cardona, Solid State Commun. **74**, 347 (1990).
[27]E. Molinari and S. de Gironcoli (unpublished).
[28]A. K. Sood, J. Menéndez, M. Cardona, and K. Ploog, Phys. Rev. Lett. **54**, 2115 (1985).
[29]T. Ruf, V. I. Belitsky, J. Spitzer, V. F. Sapega, M. Cardona, and K. Ploog, Phys. Rev. Lett. **71**, 3035 (1993).